PCCP

Accepted Manuscript

ROYAL SOCIETY OF CHEMISTRY

www.rsc.org/pccp

One-Dimensional Ionic Self-Assembly in a Fluorous Solution: The Structure of Tetra-*n*-butylammonium tetrakis[3,5-bis(perfluorohexyl)phenyl]borate in Perfluoromethylcyclohexane by Small-Angle Neutron Scattering (SANS)

Kenneth A. Rubinson [a,b,*], Philippe Bühlmann[c], Thomas C. Allison[d]

a. NIST Center for Neutron Research, National Institute of Standards and Technology, Gaithersburg, MD 20899
b. Department of Biochemistry and Molecular Biology, Wright State University, Dayton, OH 45435
c. Department of Chemistry, University of Minnesota, 207 Pleasant St. SE, Minneapolis, MN 55455, USA,
d. Computational Informatics Research Group, Material Measurement Laboratory, National Institute of Standards and Technology, Gaithersburg, MD 20899

Authors= emails: Rubinson@nist.gov
buhlmann@umn.edu
thomas.allison@nist.gov

Key words: SANS, non-conducting ionic solution, perfluorocarbon solvent, fluorous

Running title: Non-conducting ionic solute structure

Abstract

Fluorous liquids are the least polarizable condensed phases known, and their nonpolar members form solutions with conditions the closest to being *in vacuo*. A soluble salt consisting of a large fluoroborate anion, tetrakis[3,5-bis(perfluorohexyl)phenyl]borate, and its counterion, tetra-*n*-butylammonium, dissolved in perfluoromethylcyclohexane produces ionic solution with extremely low conductivity. These solutions were subjected to small-angle neutron scattering (SANS) to ascertain the solute structure. At concentrations of 9 % mass fraction, the fluorophilic electrolyte forms straight, long (>160 Å) self-assembled structures that are, in essence, long, homogeneous cylinders. Molecular models were made assuming a requirement for electroneutrality on the shortest length scale possible. This shows a structure formed from a stack of alternating anions and cations, and the structures fit the experimental scattering well. At the lower concentration of 1 %, the stacks of ion pairs are shorter and eventually break up to form solitary ion pairs in the solution. These characteristics suggest such conditions provide an interesting new way to form long, self-assembling ionic nanostructures with single-molecule diameters in free solution onto which various moieties could be attached.

Abbreviations:

SLD scattering length density
SANS small-angle neutron scattering
TBA tetra *n*-butylammonium ion
PTFE polytetrafluoroethylene
ISE ion-selective electrode
M molar (moles L^{-1})

Introduction

Fluorous solvents (that is, perfluorocarbon solvents) with their low polarizabilities possess extremely weak van der Waals forces between their molecules, which makes them the most nonpolarizable solvents known.[1-3] Because of their extraordinarily low polarity, they are immiscible with many common organic solvents,[4, 5] and C-6 and longer perfluoro groups are generally required to obtain moderate solubilities.[4, 6] Another viewpoint considers the fluorous phases to provide conditions not unlike those of a gaseous phase or the vacuum. For example, optical spectra of solutes in fluorous solvents closely resemble their spectra in the gas phase.[7]

Fluorous phases have shown exceptional properties for electroanalytical chemistry as superior sensing membranes for ion-selective electrodes. Potentiometric sensors with fluorous cation-selective membranes exhibit a selectivity range that can be eight orders of magnitude wider than those of comparable conventional sensors, which can be explained by the exceptionally poor solvation of ions in fluorous phases.[8] For example, pH sensors with a selectivity for H^+ over Na^+ exceeding 10^{13}:1 have been prepared.[9] Similarly, selectivities of fluorophilic ionophores for Ag^+ and for CO_3^{2-} exceed non-fluorous ISEs by several orders of magnitude.[10-12] Only the introduction of the title compound, tetrabutylammonium tetrakis(3,5-bis(perfluorohexyl)phenyl)borate, as electrolyte permitted the first ever voltammetry with an undiluted perfluorocarbon as solvent.[13]

The solution conductivity of the title compound, with the chemical structure illustrated in Figure 1, was found to be extremely low. In addition only a minor change in dielectric permittivity occurred compared to the pure solvent. This result was assumed to be due to strong ion pairing.[14] Similar molecular association driven by fluorous solvent properties have been utilized to drive 3-D and 1-D associations to specific structures.[2, 15, 16]

To find the solute structure, the solutions were subjected to small-angle neutron scattering (SANS), since SANS probes structures from the 10 Å to 1000 Å length scale. (10 Å = 1 nm.) We have found that at mass fraction 9 %Bequal to a 52 mM solution of the saltB the ions form long (> 160 Å), stiff chains. Structure modeling suggests the nanorods self-assemble in the form of alternating anions and cations with the perfluoroalkane chains arrayed perpendicularly to the long axis. Only the outer part of these are chains accessible to the solvent. On the other hand, in 1 % mass fraction solutions (5.8 mM), the ions many days after dilution apparently exist as monodisperse ion pairs.

Materials and Methods[¤]

Samples

Besides the solvent alone for background subtraction, three samples were run consisting of nominally 1 % and 9 % mass fraction of the salt in perfluoromethylcyclohexane. The salt was prepared as described by Olson et al.,[14] with the solutions prepared by weighing the two components. The solvent density is 1.788 g/mL at 25 °C[17] and 1.799 at 20 °C,[18] and the formula weight of the salt is 3105.97 Da. As a result, the 1 % and 9 % solutions are approximately 5.8 mM and 52 mM.

Origins of the Scattering

The neutron scattering arises due to contrast between the solvent and the scattering particles at the wavelength used. The contrast can be calculated from the scattering per unit volume of the solution, which is the scattering length density (SLD), ρ. The experimental contrast is $(\Delta\rho)^2 = (\rho_{particle} - \rho_{solvent})^2$. Since the neutron scattering lengths for the isotopes are known, the calculation then requires the mass densities of the components. The required values are listed in Table 1. In the table, the negative value arises because hydrogen has a negative scattering length, while deuterium, carbon, nitrogen, and most other nuclei possess positive values. This sign variation indicates a change of phase of the scattering.[19]

The densities for the TBA and the borate ions utilize the ionic partial molar volumes measured in four solvents by Krakowiak et al. [20] and the formula weights. They vary little with solvent identity. From the values in the table, the SLDs of the solution components and substructures were estimated using the calculator at www.ncnr.nist.gov/resources/sldcalc.html.

The calculator finds the scattering length density from the sum of the scattering lengths of the atoms and the expected density of the molecule or molecular part. In effect, the calculation is a measure of the volume fraction with the amount of scattering from the sum of the atoms in that volume fraction. To the extent that the scatterers in fact occupy a larger volume, the scattering length density decreases. As will be discussed below, the borate fluorocarbon chains do, indeed, occupy a larger volume than expected from a liquid or solid fluorocarbon. Their scattering length density is, then, decreased and they exhibit a much larger contrast with the solvent than calculated from the values in the table.

SANS measurements

SANS measurements were performed on the NG3 30 meter SANS instrument at the NIST Center for Neutron Research (NCNR) in Gaithersburg, MD[21]. The substituted ammonium-borate salt solutions were measured in tightly sealed silica cells with 1 mm pathlengths using neutrons with $\lambda = 6$ Å and $\Delta\lambda/\lambda = 0.11$. Scattered neutrons were detected with a 64 cm × 64 cm

two-dimensional position sensitive detector with (128 ×128) pixels and 0.5 cm resolution per pixel. Data reduction was accomplished using Igor Pro software (WaveMetrics, Lake Oswego, OR) with SANS macros developed at the NCNR[22]. Raw counts were normalized to a common monitor count and corrected for empty cell counts, ambient room background counts, and non-uniform detector-pixel response. Data were placed on an absolute scale by normalizing the scattering intensity to the incident beam flux for each individual pixel. Finally, the data were radially averaged to produce the scattering intensity $I(q)$ to plot as log $I(q)$ versus log q curves where $q = (4\pi/\lambda) \sin\theta$, and 2θ is the scattering angle measured from the axis of the incoming neutron beam. The sample-to-detector distance was 1.0 m, which produces a scattering range of $0.04\ \text{Å}^{-1} < q < 0.56\ \text{Å}^{-1}$, the length range equivalent of which is $160\ \text{Å} > d > 11\ \text{Å}$, as found using the relationship $d = 6.28/q$. However, the data is not reliable at q / $0.5\ \text{Å}^{-1}$ (equivalent to d . 12.5 Å) mostly because of camera geometry used here.

Both fluorine and boron absorb neutrons and activate to radioactive species that decay during the experiment times (around 15 minutes/sample). With a 20 % natural abundance, ^{10}B is activated to produce ^{7}Li and ^{4}He, and the ^{7}Li reacts further with neutrons to produce ^{4}He and radioactive ^{3}H. The ^{19}F activates with two reactions, ^{19}F (n,2n)^{18}F and ^{19}F (n,γ)^{20}F. The ^{20}F further decays to ^{20}Ne. Given the high fluorine concentration and in light of the possibility of the atomic transformations and the subsequent possible molecular decompositions, the scattering data for each sample was collected for a number of five minute durations, each period stored separately, and then all summed to provide the final scattering curves. For the beam flux at the sample, no significant decomposition was observed during the collection period for any of the samples as would be seen by a decrease in the scattering intensity outside of the counting uncertainty.

SANS Data Analysis

The background-subtracted scattering intensity from a solution can be represented by the equation

$$I(q) = n\,(\Delta\rho)^2\,V^2\,P(q)\,S(q) \qquad (1)$$

where n is the scatterers' number density, V is the scattering particle=s volume, and $(\Delta\rho)^2 = (\rho_{particle} - \rho_{solvent})^2$ is the contrast. $P(q)$ is known as the form factor, and it depends on the shape of the molecule or molecular aggregate that is scattering. In other words, $P(q)$ results from the *intra*molecular scattering arising from the solute shapes. $P(q)$ can be calculated as a simple shape, such as a sphere or cylinder, or it can be calculated from atomic coordinates such as those from an x-ray crystal structure and can be modeled by theoretical techniques such as molecular dynamics.[23] By the usual definition, at $q = 0$, $P(0) = 1$.

$S(q)$ is the *inter*particle structure factor. It serves the same purpose as $P(q)$ but for

scattering of points on different solutes. Whether interparticle scattering appears depends on the scatterers= relative positions in the solution as well as how well they stay in the same relative intermolecular positions. If they remain relatively fixed in position, $S(q)$ effects may be seen as a peak in the $I(q)$ versus q curves. In addition, the scattering magnitude will not be proportional to the concentration. However, no peak will appear if the molecules are randomly distributed in the solution. This random distribution can occur for two reasons: first, the solute particles have no interaction energy, and second, even though they are fixed, the relative structures are random and uncorrelated. If no intermolecular scattering appears, then $S(q) = 1$ for all q values. In that case, equation 1 reduces to

$$I(q) = n\,(\Delta\rho)^2\,V^2\,P(q) \qquad (2)$$

and the background-corrected scattering curves can be used directly to model the shape of the scattering units. We observed no evidence of an $S(q)$ interaction peak in either the 1 % or 9 % mass-fraction solutions of the title compound. As a result the shape and the value of the contrast are the structural variables used in the least-squares fit of the scattering curves.

The background consists of coherent and incoherent scatter from all the materials in the beam, e.g., the solvent in its silica cuvette.[24] The solvent scattering was subtracted from each solution as its fractional volume times the pure solvent's scattering curve.

Incoherent scattering in these ionic solutions arises from the naturally most abundant isotopes of hydrogen, nitrogen, fluorine, and boron. The incoherent scatter was linearly proportional to the concentrations of salt as determined from the average values of the scattering intensity measured for $0.3 < q < 0.4$. First, the solvent scattering was subtracted from each solution as its fractional volume times the pure solvent's scattering curve. Then, a correction for the solute incoherent scattering made the high-q ends of the scattering curves for both concentrations coincide.

Fitting curves

The scattering curves were fit using the IGOR program with SANS macro routines developed at the NCNR.[22] The log-log slope of the low-q side of the scattering from the 9 % solution indicates that a limited set of models that have long, straight, essentially one-dimensional structures would fit the data. Since the calculated contrast between the fluorocarbon chains and solvent is so small as can be seen from Table 1, a fit was tried with a homogeneous, circular cylinder that had the expected radius and contrast of the hydrogen-containing core. It did not fit the data well. After the computational chemistry calculations were done, well fitting results with the radii and contrasts of a core-shell cylinder (macro CoreShellCylinder) followed directly from length measurements of the resulting stacked, ion-paired structure.

DFT Stucture Modeling Calculations

In order to study the geometry of the TBA-borate ion complex, calculations were performed using the semiempirical PM7 computational chemistry method.[25] This method was appropriate for this study since it yields valid geometries and runs 10^2 to 10^3 times faster while permitting treatment of much larger systems than other common methods such as density functional theory. All calculations were carried out using the MOPAC2012 computational chemistry code (Stewart Computational Chemisty, Colorado Springs, CO).

Optimization (*i.e.*, finding a stationary point on the potential energy surface) of the TBA-borate ion complex was performed in several stages. First, the TBA and borate ions were separately optimized. Second, a TBA-borate ion pair was formed first by placing the two ions in close proximity manually. A number of initial geometries of the ion pair were optimized, and this lowest energy structure was used in subsequent optimizations. Finally, the pairs were stacked, and the resulting complexes containing from two to eight TBA-borate ion pairs were optimized. Optimizations were performed using the MOZYME option and the BFGS optimizer in the MOPAC2012 code with the Aprecise@ option. The effect of the perfluoromethylcyclohexane solution was incorporated via the conductor-like screening model (COSMO) method [26] with a dielectric constant $\varepsilon = 1.86$ and a solvent radius of 1.3 Å as recommended in the MOPAC2012 manual. (Note that this is not the actual radius of the solvent.) The largest structure optimized contains 8 complexes (1936 atoms) approximately 100 Å long. This structure is discussed further in the next section together with various distances within it that are listed in Table 2.

The solvent accessible surface illustrations seen in Figure 3 were made using Chem3D (PerkinElmer Informatics, Waltham, MA). The sphere-equivalent radius of 4.26 Å for perfluoromethylcyclohexane was derived from its FW of 350.0 Da and the density of the neat liquid of 1.787 g cm^{-3} leading to a molecular volume of 325 $Å^3$/molecule. The sphere of radius 4.26 Å fits that molecular volume.

Results and Discussion

Analysis of the 9 % solution scattering

The title fluorophilic electrolyte is soluble in perfluoromethylcyclohexane to greater than 80 mM. Solutions of ions of similar composition and concentration still have low conductivityBin the 3 μS cm^2 $equiv^{-1}$ range (KCl in water, 150 S cm^2 $equiv^{-1}$)Bwhich suggests relatively strong ion aggregation occurs. However, as seen in Figure 2 and Table 3, the SANS scattering of the solution at the low-*q* side of the log-log curve has a straight-line slope of -1. This is characteristic of a long, stiff cylinder.[27-30]

Initial modeling as a simple cylinder showed that such a geometrical shape is reasonable,

but the best-fit radius of about 10 Å was much larger than expected from the SLDs (Table 1) for a self-assembled structure that was, as noted in the Methods section, calculated to have a high contrast for the hydrogen-containing core and much lower contrast for the peripheral perfluoroalkane chains within the fluorous solvent. In order to get a clearer understanding, a molecular structure was calculated as described in the Methods section. Various ways of pairing the ions were tried, and the final structure of a section of the self-assembled nanorod *in vacuo* (an octomer of pairs) is shown in Figure 3. Various distances within this structure are listed in Table 2.

Inspection of the structure shows why the scattering structure extended to the outer cylinder edge radius; the solvent cannot penetrate toward the core much beyond the outer ends of the fluorocarbon side chains and only within the wider of the two, unevenly open clefts. The effective contrast of the fluorocarbons also is lower because they fill only about a quarter of the volume outside of the proton-containing core; that is, about half of the radial space and half of the volume along the axis. See Figure 3.

The molecular model's measurements listed in Table 2 were used for a cylinder model with a core radius of about 5 Å of SLD (1.1×10^{-6}) $Å^{-2}$ inside a surrounding shell with thickness of (24 - 10)/2 = 7 Å. Outside of the shell, the SLD was held at that of the solvent. These SLDs are listed in Table 1. The best fit with these starting points finished with the values in Table 3 for the 9 % solution.

The best fit agrees with the long, stiff, self-assembled construct suggested by the computational results. The final SLD of the shell containing the fluoroalkane chains was much smaller the "filled" value of (4.76×10^{-6}) $Å^{-2}$. As seen in Figure 3, the structural reason that the modeled shell has so much contrast with the solvent is that the perfluoromethylcyclohexane cannot penetrate much past the ends of the fluoroalkane chains, and the volume is, in effect, partially empty. Further, we expect that given the chains have open space between the ring-attached pairs, the chain ends are flexible and could fill the space to exclude even more of the volume to the solvent than is illustrated in the figures.

Note that the great length of the assembly suggested by the curve fitting is not able to be validated unless the full length can be included within the q range within scattering window. However, we can say that it is certainly much longer than 160 Å, which corresponds to 15 ion pairs.

The stiffness of the chain within the range of the data window was further tested by fitting to a wormlike chain model. The Kuhn length (= 2 × persistence length) remained one-third to one-half the contour length, which suggests that stiff is a reasonable label for the structure under the experimental conditions.

Analysis of the 1 % solution scattering

The long assembly does not persist in the 1 % solution. A much shorter structure was evident a few days after the solution was made. After nine weeks at ambient temperature (~22 C), when a second measurement on the same solution was made, the fluorophilic electrolyte reached an apparent equilibrium where it exists as solitary ion pairs. The scattering obtained from the solutions both at the earlier and later times are shown in Figure 4.

At the earlier time, the 1 % solution curve appears much like the 9 % solution, and the same strategy was used for fitting. The results listed in Table 3 indicate a shorter assembly that is similar in cross section. However, because of the lower signal-to-noise, we expect the values not to be as accurate as those for the 9 % solution. However, the average length, even with its broad uncertainty, is significantly shorter than in the more concentrated solution.

Clearly, by comparison of the two curves shown in Figure 4, the structure changed significantly. The same core-shell cylinder model was used, but the interplay of the variables allowed a wide range of values to produce similar fits. The interdependence of the shell thickness and shell SLD was particularly strong. In order to obtain reasonable convergence, the shell SLD was held to that of a solid perfluoroalkane. The most important value is the best-fitting length of 7.8 Å for the now-thin cylinder. This is in moderate agreement with the molecular model's 9.9 Å between the outside limit of the ammonium butyl chains to the *p*-proton's position on the phenyl ring along the B-N axis of the solitary ion pair, as illustrated in Figure 5.

In addition, the much reduced thickness of the shell appears to be reasonable since within an ion pair, the fluorocarbon chains are accessible to the solvent, unlike along the much longer assembly. This can be interpreted as creating a near match in SLDs between the solvent and the outer part of the chains, which makes them appear to be shorter since SLD-matched structures are not expected to contribute much to the scattering.

Conclusions

Tetrakis[3,5-bis(perfluorohexyl)phenyl]borate, and its counterion, tetra-*n*-butylammonium, were dissolved in perfluoromethylcyclohexane making a non-conducting solution. At concentrations of 9 % mass fraction, the salt forms straight, long (>>160 Å) self-assembled structures that are a single molecule wide. Computational structure results that agree with SANS measurements show a complex formed from a stack of alternating anions and cations, and from which the solvent is significantly excluded. At the lower concentration of 1 %, the stacks of ion pairs eventually break up to form solitary ion pairs in the solution. These characteristics suggest such conditions provide an interesting new way to form long, self-assembling ionic nanorods with single-molecule diameters onto which various moieties could be attached that exist in a solvent that is easily removed.

Table 1. Calculated scattering length densities.[a]

Scatterer I.D.	Physical density /(g cm^{-3})	ρ (calculated[b] scattering length density/$Å^{-2}$)
Solvent (C_7F_{14})	1.79	3.87 E-6
perfluorohexyl group (PTFE density)	2.16	4.76 E-6
TBA ($C_{16}H_{36}N^+$)	0.85[c]	-0.40 E-6
borate no perfluoro groups ($BC_{24}H_{12}$)	1.14[c]	4.62 E-6
core TBA-$BC_{24}H_{12}$ volume average	0.99_5[c]	1.10 E-6

a. Abbreviations: TBA = Tetra-*n*-butylammonium; PTFE = polytetrafluoroethylene

b. http://www.ncnr.nist.gov/resources/sldcalc.html

c. From partial molar volume data of Krakowiak et al.[20]

Table 2. Distances within the calculated eight-pair structure perpendicular to long axis[a]

F to F between opposite chain ends	24 Å
Between opposite borate para-hydrogens	8.9 Å
CH_3 to CH_3 at opposite amine chain ends	11.7 Å
(B-B and N-N next neighbor along axis)	10.9 Å
p-hydrogen to outer butyl hydrogen along parallel to N-B axis within adjacent salt pair	9.9 Å

a. Nucleus to nucleus distances

Table 3. Fitting variables for core-shell cylinder[a]

Solution	Core Radius/Å	Shell Thickness/Å	Cylinder Length/Å	Shell SLD H 10^6 /Å^2	Low-*q* log-log slope
1%	6 ± 3	11 ± 3	56 ± 27	0.8 ± 5	-1.1 ± 0.33
1% later	5.84 ± 0.06	2.25 ± 0.02	7.8 ± 0.2	4.76 held[b]	- -
9 %	5.2 ± 0.1	5.7 ± 0.1	(4 ± 0.4) H 10^3	0.8 ± 0.4	-1.03 ± 0.07

a. The uncertainties are standard deviations for the best-fit variables with others held constant. The core SLD was held at (1.1×10^{-6}) Å^{-2}, and the solvent SLD was held at (3.87×10^{-6}) Å^{-2}.

b. The shell thickness and shell SLD are strongly coupled. This was held at the PTFE value.

Figure Captions

Figure 1. Tetra-n-butylammonium tetrakis[3,5-bis(perfluorohexyl)phenyl]borate

Figure 2. The SANS scattering curve for the 9 % solution and the best fitting curve of the core-shell model. The uncertainties (± σ) are for the counting statistics only.

Figure 3. The molecular structure of a model the eight pairs in length of the TBA-borate complex shown end on (left) and lengthwise and showing the limits of solvent accessibility (grey cloud) for a static structure. Even for the static structure, the solvent can penetrate only slightly past the outer edge. That together with flexibility at the ends of the chains reduces the apparent diameter for the scattering.

Figure 4. The SANS scattering curves of the 1 % TBA-borate solution a few days after mixing (top) and after more than a month of equilibration (bottom). The uncertainties (± σ) are for the counting statistics only.

Figure 5. Image of a solitary ion pair from the eight-pair model. The arrow length is 9.9 Å. Note the pairings of the sidechains from different rings.

Disclaimer

Certain commercial materials are identified in this paper, but such identification does not imply recommendation or endorsement by the National Institute of Standards and Technology, nor does it imply that the materials or equipment identified are necessarily the best available for the purpose.

References

1. J. A. Gladysz, D. P. Curran and I. T. Horváth, *Handbook of Fluorous Chemistry*, Wiley & Sons, New York, 2005.
2. J.-M. Vincent, *J. Fluor. Chem.*, 2008, **129**, 903-909.
3. K. L. O'Neal and S. G. Weber, *J. Phys. Chem. B*, 2009, **113**, 149-158.
4. E. de Wolf, G. van Koten and B.-J. Deelman, *Chem. Soc. Rev.*, 1999, **28**, 37-41.
5. Q. Chu, M. S. Yu and D. P. Curran, *Tetrahedron*, 2007, **63**, 9890-9895.
6. E. G. Hope and A. M. Stuart, *J. Fluor. Chem.*, 1999, **100**, 75-83.
7. C. Laurence, P. Nicolet, M. T. Dalati, J.-L. M. Abboud and R. Notario, *J. Phys. Chem.*, 1994, **98**, 5807-5816.
8. P. G. Boswell and P. Bühlmann, *J. Am. Chem. Soc.*, 2005, **127**, 8958-8959.
9. P. G. Boswell, C. Szíjjártó, M. Jurisch, J. A. Gladysz, J. Rábai and P. Bühlmann, *Anal. Chem.*, 2008, **80**, 2084-2090.
10. C.-Z. Lai, M. A. Flerke, R. C. da_Costa, J. A. Gladysz, A. Stein and P. Bühlmann, *Anal. Chem.*, 2010, **82**, 7634-7640.
11. L. D. Chen, D. Mandal, G. Pozzi, J. A. Gladysz and P. Bühlmann, *J. Am. Chem. Soc.*, 2011, **133**, 20869-20877.
12. M. A. Maurer-Jones, M. P. S. Mousavi, L. D. Chen, P. Bühlmann and C. L. Haynes, *Science*, 2013, **4**, 2564-2572.
13. P. G. Boswell, E. C. Lugert, J. Rabai, E. A. Amin and P. Bühlmann, *J. Am. Chem. Soc.*, 2005b, **127**, 16976-16984.
14. E. J. Olson, P. G. Boswell, B. L. Givot, L. J. Yao and P. Bühlmann, *J. Electroanal. Chem.* , 2010, **639**, 154-160.
15. P. Metrangolo, H. Neukirch, T. Pilati and G. Resnati, *Acc. Chem. Res.*, 2005, **38**, 386-395.
16. C. B. Aakeröy, J. Desper, B. A. Helfrich, P. Metrangolo, T. Pilati, G. Resnati and A. Stevenazzi, *Chem. Comm.*, 2007, 4236-4238.
17. N. V. Lifanova, T. M. Usacheva and V. I. Zhuravlev, *Russian J. Phys. Chem.* , 1992, **66**, 125-126.
18. R. D. Fowler, J. M. Hamilton, J. S. Kasper, C. E. Weber, W. B. I. Burford and H. C. Anderson, *Ind. & Engin. Chem.*, 1947, **39**, 375-378.
19. R.-J. Roe, *Methods of X-Ray and Neutron Scattering in Polymer Science*, Oxford Univ. Press, Chap. 1., New York, 2000.
20. J. Krakowiak, D. Bobicz and W. Grzybkowski, *J. Mol. Liquids*, 2000, **88**, 197-207.
21. C. J. Glinka, J. G. Barker, B. Hammouda, S. Krueger, J. J. Moyer and W. J. Orts, *J. Appl. Cryst.*, 1998, **31**, 430-445.
22. S. R. Kline, *J. Appl. Cryst.*, 2006, **39**, 895-900.
23. J. E. Curtis, S. Raghunandan, H. Nanda and S. Krueger, *Comp. Phys. Comm.*, 2012, **183**, 382-389.
24. K. A. Rubinson and J. Hubbard, *Polymer*, 2009, **50**, 2618-2623.
25. J. J. P. Stewart, *J. Mol. Model.*, 2013, **19**, 1-32.

26. A. Klamt and G. Schüürmann, *JCS Perkin 2*, 1993, **2**, 799-805.
27. P. W. Schmidt, *J. Appl. Cryst.*, 1982, **15**, 567-569.
28. P. W. Schmidt, *J. Appl. Cryst.*, 1991, **24**, 414-435.
29. B. Hammouda, *J. Appl. Cryst.*, 2010, **43**, 716-719.
30. B. Hammouda, Probing Nanoscale Structures – The SANS Toolbox, Chap. 22. www.ncnr.nist.gov/staff/hammouda/theSANS toolbox.pdf

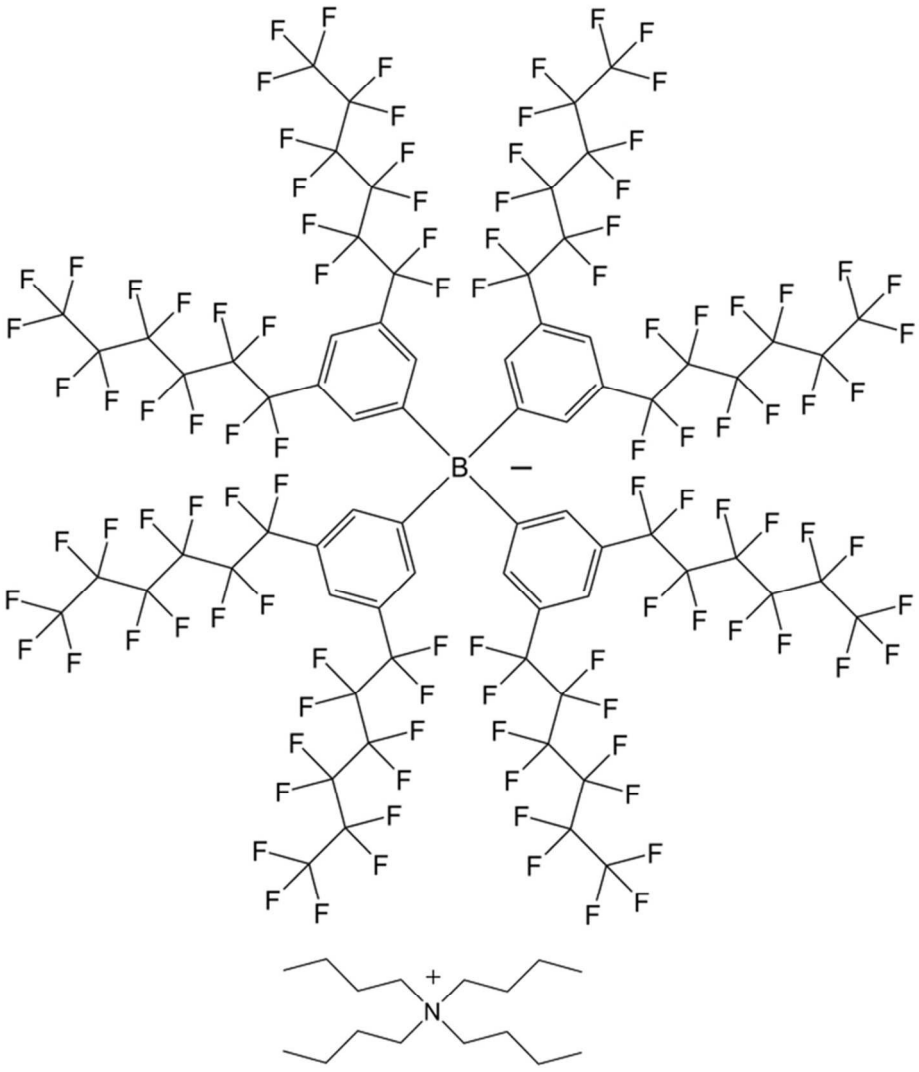

92x102mm (300 x 300 DPI)

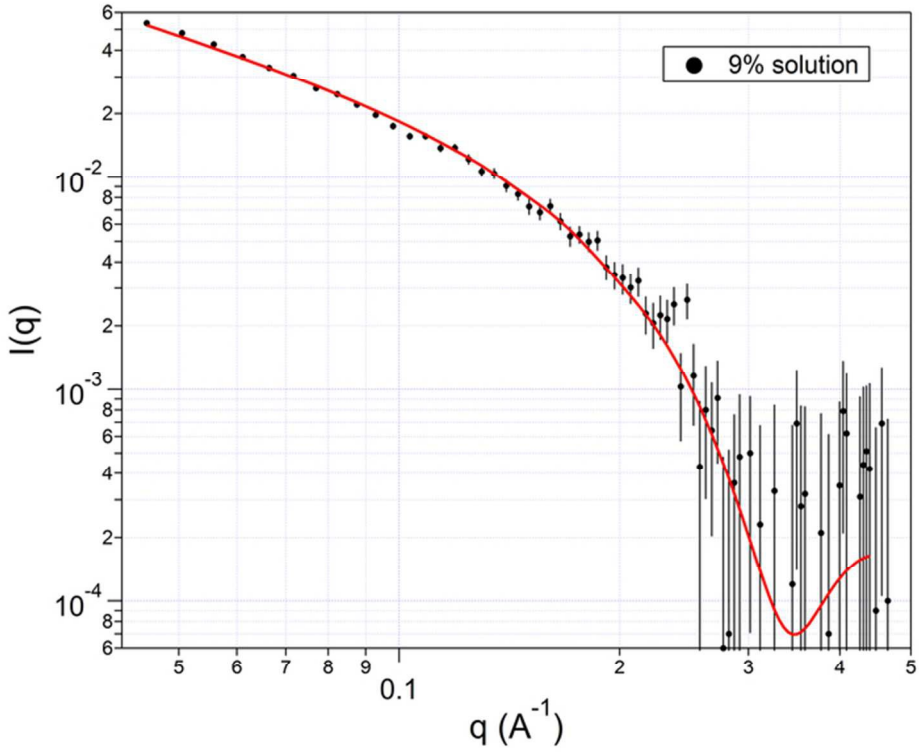

64x50mm (300 x 300 DPI)

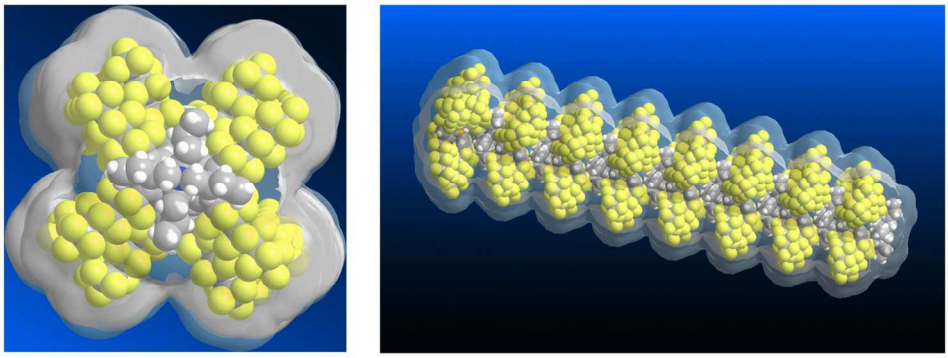

434x177mm (300 x 300 DPI)

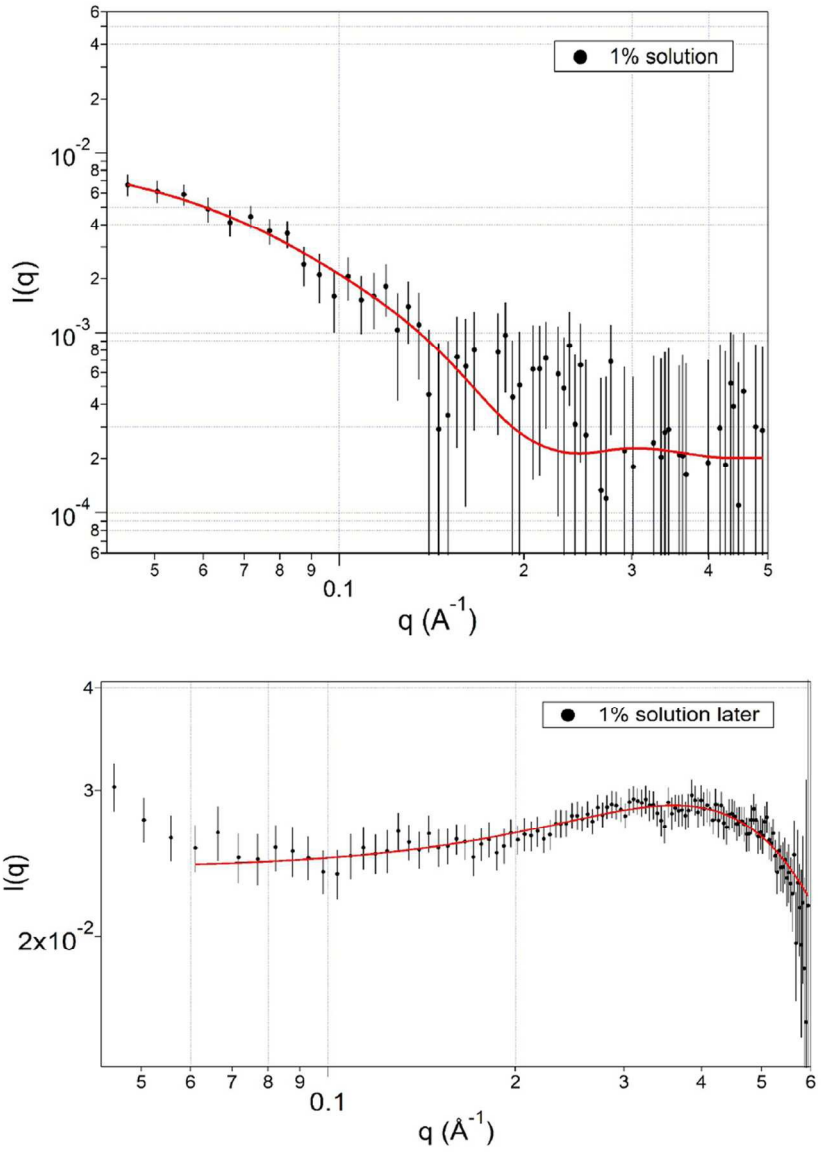

115x160mm (300 x 300 DPI)

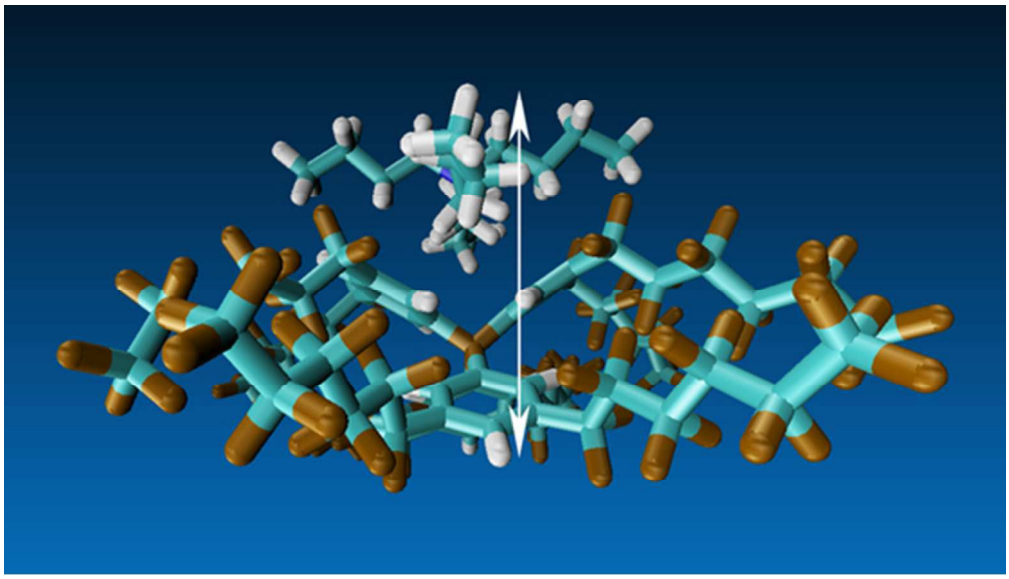

47x26mm (300 x 300 DPI)